Valuable Experimental Model of Contraction Pneumatic Muscle Actuator

Alaa Al-Ibadi
University of Salford
Computing, Science and Engineering
a.f.a.al-ibadi@edu.salford.ac.uk

Samia Nefti-Meziani
University of Salford
Computing, Science and Engineering
S.Nefti-Meziani@salford.ac.uk

Steve Davis
University of Salford
Computing, Science and Engineering
S.T.Davis@salford.ac.uk

***Abstract*— modelling of pneumatic muscle actuators "PMA" is one of the valued challenges in soft robotic researches, which is still under modification for the McKibben artificial muscle. Accurate force, length and position models allow for the wide use of make the continuum robot arm in industrial and medical applications. Moreover, accurate control can be achieved. This paper presents new formulas to model the length of contraction PMA. The sigmoidal shape of contraction length characteristics makes the sigmoid function a suitable form to model, which its coefficients depend on the nominal length "L_0". Furthermore, we modified the existing force model by calculating the most affected parameters. Then we are modelling the angle of the arm. The three proposed models make it easy to track the length (position), the force of PAMs and position angle of PMA arm.**

***Keywords*— Contraction PMA, Experimental Model, Force Formula, Pneumatic Muscle Actuator, bending angle.**

I. INTRODUCTION

Many researchers have used numerous types of actuators for industrial and medical applications including electrical, magnetic, hydraulic and pneumatic muscle actuators (PMA) [1-4]. The wish to enhance the behaviour of robots by making them safer for human interaction in both industrial and medical areas resulted in an increase of interest in PMA [3, 5]. In recent years, there have been a substantial increase in designing, modelling and constructing (biological based) continuum robots [6-9].

The PMA has positives over classical pneumatic cylinders such as high power to weight ratio, low workspace requirement, flexible structure [1, 4, 5, 10-12], infinite degrees of freedom (DOF) [13-15], variable installation options, no mechanical wear, slight compressed-air consumption, availability of dimension, low cost and robust reliability for human used [5, 12]. A part from these advantages, PMA has been regarded as a suitable substitutive for other actuators such as electrical and hydraulic [3, 4]. Furthermore, the robot is expected to be safer and more flexible [2, 5, 11]. Despite its observable advantages, PMA exhibits highly nonlinear features [3, 11, 12, 16-19], which are time dependent. The presenting of nonlinearity in the PMA is due to the compressibility of air, the inner tube elastic-viscous properties and geometrically compound behaviours of the PMA outer covering [1, 5, 11]. Moreover, the hysteresis behaviour is caused by the inner tube, which produces different characteristics of PMA during contracting and expanding [6, 10, 12]. These make the modelling and controlling of pneumatic muscles more difficult [1, 4, 5, 20, 21]. Current models do not fully explain every stage of the mechanical performances well; therefore, an enhanced model is still required [5]. Different models have been proposed to describe the behaviours of the PMAs. Among these models, the Chou and Hannaford model [22] and the Tondu and Lopez model [17] are widely used. These models are based on the assumption of the virtual works of the cylindrical shape and the small thickness of the inner tube [1, 17, 22]. Even though they are excellent initial descriptions of the mechanical behaviours, these models are still limited in predicting the performance of the PMA, at least in no-load situations. Also, the force of pulling, length change, air pressure supply, radius and material properties are the major parameters of the PMA and dynamic performances. Moreover, the relationships between these parameters are greatly changed from one PMA to another.

Most modelling methods act with the force of PMA due to changing in pressure input and the PMA volume. On the other hand, the model for length changing is still under research, including mathematically. In this paper, we constructed a contractor PMAs with different lengths to study its performances, and we have written a set of mathematical equations to model change of length with pressure input. In addition, we studied the parameters that enhance the force model formula and modelled the position angle of the arm.

II. CONTRACTOR PMA

Depending on the construction of the pneumatic muscle actuator, there are two types of muscles: contractor and extensor artificial muscles. Fig.1 shows the photograph of a 20cm contractor PMA. Generally, the PMA is constructed from an inner rubber tube which is covered by a braided sleeve with two plastic (or any solid material) terminals which are strongly fixed by cable ties. One of the terminals has a

small hole for input and output of actuated air. Fig.2 shows a basic diagram of PMA with "L" length, "D" diameter and "θ" angle between the vertical axis and braided strand.

Fig.1 A photograph of a 20 cm PMA

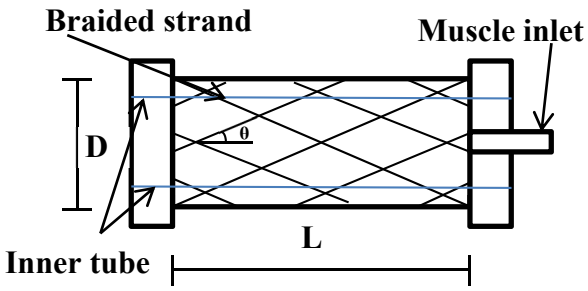

Fig. 2 Pneumatic muscle actuator diagram

The contraction performance of PMA occurs when the braided angle "θ" is less than 54.7° [22, 23]. Percentage of contraction differs from one muscle to another but does not exceed 35% [2, 16, 17].

III. MODELLING OF CONTRACTION LENGTH

The sigmoidal shape [16] of muscle length as is shown in Fig.3, leads to modelling the length of PMA performance as a mathematical sigmoid function. To modelling the length with input air pressure, five muscles are used for nominal lengths "L_0" (15, 20, 25, 30 & 40 cm). For each muscle, we have studied and recorded with a pressure gauge "P", how its length changed. Fig.3 shows three PMAs with three nominal lengths (20, 30, and 40 cm) and it is clear that there is a significant matching between experiment and model plots. From this pneumatic muscles data, we define a set of equations depending on "L_0 and p". Equation (1) describes the length of the pneumatic muscle with both (p & L_0), and equation (2) gives the parameter values of eq. (1), depending on the nominal length of the PMA (L_0).

$$L = a + \frac{b}{[1+(\frac{p}{c})^d]^e} - 0.009L_0\sqrt{p} \qquad (1)$$

$$\text{Where: } \begin{bmatrix} a \\ b \\ c \\ d \\ e \end{bmatrix} = \begin{bmatrix} 0.4351 & 0 & 0.0183 & -0.0003 \\ 0.5649 & 0 & -0.0183 & 0.0003 \\ -0.0141 & 0 & 0.0031 & -0.00006 \\ 0.5487 & 0 & -0.0136 & 0.00007 \\ 0 & 0.3694 & 0 & 0 \end{bmatrix} \begin{bmatrix} L_0 \\ L_0^{0.75} \\ L_0^2 \\ L_0^3 \end{bmatrix} \qquad (2)$$

The sigmoidal function firstly considered for each muscle individually, then we added ($-0.009L_0\sqrt{p}$) as an error correction.

The final step is finding the parameters (a, b, c, d and e) as a function of L_0.

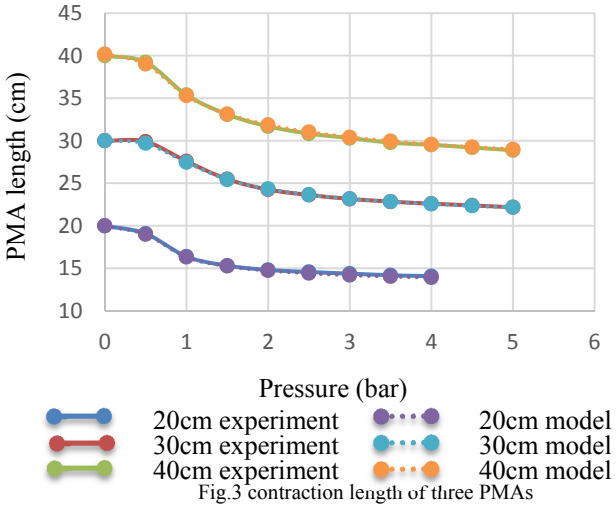

Fig.3 contraction length of three PMAs

IV. MODELLING OF PULLING FORCE

The muscle actuator converts the pneumatic energy into mechanical form by transferring the pressure input to the muscle into the contracting force [5, 24]. The changing of input work (w_{in}) of the pneumatic muscle is:

$$dw_{in} = p.dv \qquad (3)$$

where, (dv) is the volume change. The output work (w_{out}) changes with change of length, as in the following equation:

$$dw_{out} = -f.dL \qquad (4)$$

Fig. 4 shows the relation between the parameters of PMA. Equations (5, 6 and 7) define the Tondu and Lopez force model under the following assumptions: 1- The shape of PMA is a perfect cylinder with zero wall thickness. 2- There is a contact between the inner rubber tube and the braided sleeve. 3- The braided strand length is constant. 4- There is no friction between the tube and the sleeve. 5- Neglecting the latex tube force [1, 17].

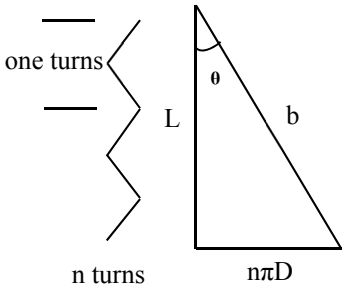

Fig. 4 parameters of PMA

Where: $L = bcos\theta, D = b\frac{sin\theta}{n\pi}$ (5)

By considering eq. (5) the strand length can be evaluated as:

$$b = (L^2 + (Dn\pi)^2)^{\frac{1}{2}} \quad (6)$$

The force "f" can be calculated as the multiplication of the gauge pressure and the volume change with respect to length.

$$f = \pi r_0^2 p[\alpha(1-\varepsilon)^2 - \beta] \quad (7)$$

Where: $\varepsilon = \frac{L_0 - L}{L_0}$, $\alpha = \frac{3}{tan^2(\theta_0)}$, and $\beta = \frac{1}{sin^2(\theta_0)}$.

The maximum value of the contraction ratio "ε" occurs when ($L=L_0$). Moreover, "r_0 and θ_0" represent the initial values of radius and angle of PMA respectively. Fig. (5) below shows the experimental force data with the plot of eq. (7) for 20cm PMA. This figure illustrates that the difference between the theoretical and experimental records has two main causes. The first one is the non-cylindrical shape of PMA at zero or low air pressure supplied. The second reason is less contact between the inner rubber tube and the braided sleeve. To overcome these two aspects, the correction factor "q(p)" [12] is used by multiplying it by the contraction ratio of eq.7.

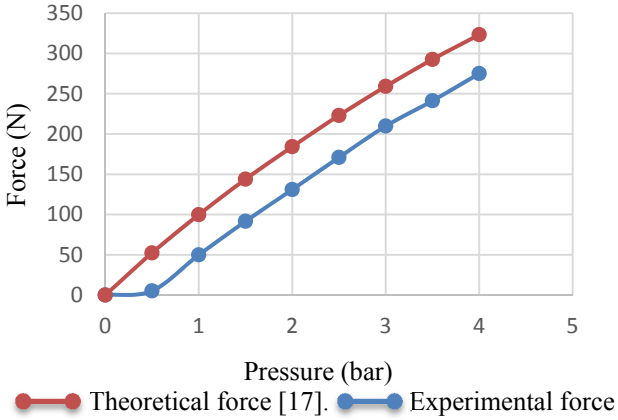

Fig.5. Force of 20cm PMA

$$q(p) = 1 + 1e^{-p} \quad (8)$$

The increase on "p" caused a decrease on "q", therefore, at high pressure the shape of PMA become perfectly cylindrical. On the other hand, the experimental data shows that the amount of useless (zero force) pressure is (0.45 bar), for that the gage pressure in eq.7 is sited by (0 bar) from (0-0.45 bar) and is shifted by (0.45 bar). The zero force pressure is studied by [25] as a function of pressure and inner tube diameter.
Taking these two factors into account gives substantial matching between the experimental and theoretical force characteristics. Fig.6 gives the force plot for three muscles under test with L_0 (20, 30 and 40 cm).
The modification of eq.7 shows in eq.9 below:

$$f = 0 \ , \ 0 \le p \le 0.45 \ bar$$

$$f = \pi r_o^2 (p - 0.45)[\alpha(1 - q\varepsilon)^2 - \beta] \ , \ p \ge 0.45 \quad (9)$$

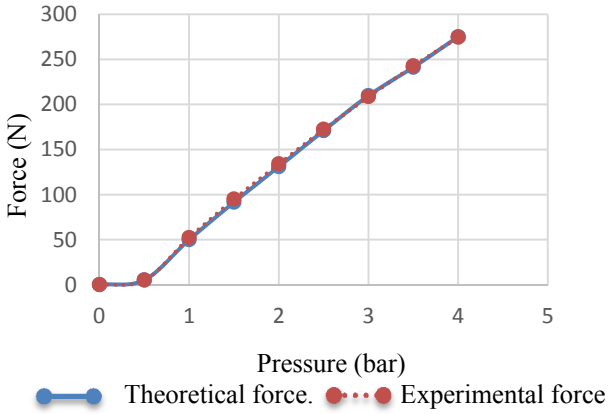

(a) Force of 20cm PMA

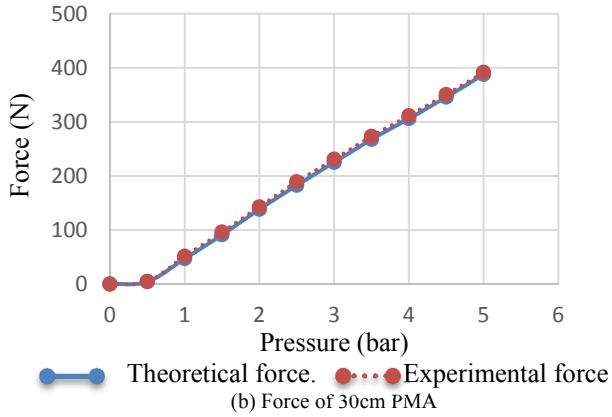

(b) Force of 30cm PMA

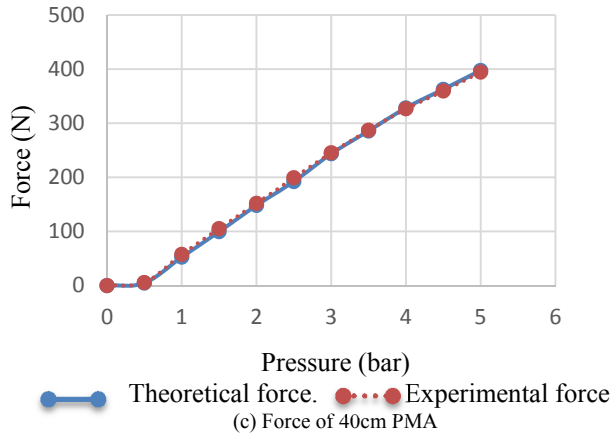

(c) Force of 40cm PMA

Fig.6. Proposed force characteristics of three different PMAs

V. PNEUMATIC MUSCLE ACTUATOR ARM

A 30 cm artificial muscle is used in the design of a continuum arm, which is constructed with four identical PMAs as in Fig.7.

Fig.7. Continuum arm of 4-PMAs

As shown in Fig.7, there is one muscle in the centre of the arm, and the other three are located as a 120º displacement. The distance between each muscle's centre and the centre of the arm is 30mm. The same tests are applied to the arm for contraction and force characteristics. Fig.8 illustrates the change in length with respect to pressure input, comparing individual muscles. The slight differences between the two plots are due to the friction between muscles. Furthermore, it is clear that the arm is acting as a single PMA for contraction characteristics whilst adding many features such as pending and multi positions of its end. With reference to eq.9, both input pressure and contraction ratio have an effect on the force of each PMA. Therefore, the expected force characteristics for the arm will be four times that of a single muscle.

.

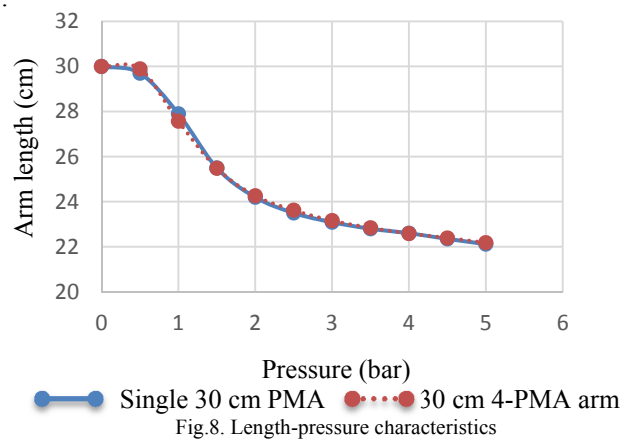

Fig.8. Length-pressure characteristics

Fig.9 clearly explains this idea. Consequently, the force of multi PMAs in parallel can be calculated as in eq.10.

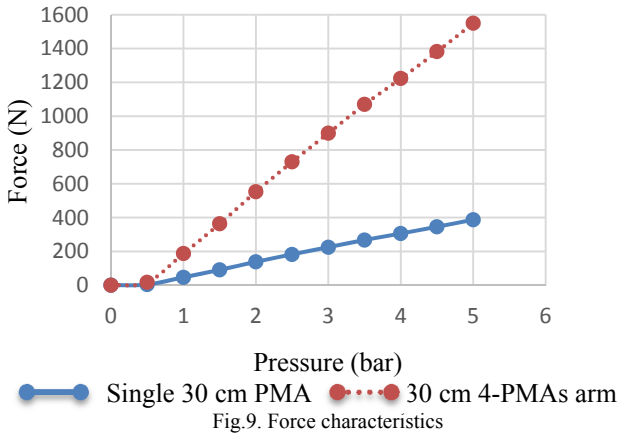

Fig.9. Force characteristics

$$F = Kf \qquad (10)$$

Where F: is the total force (N), K: is the number of parallel muscles, and f: is the force of single muscle (N).

To explain this idea more clearly, two PMAs in series are used to test the force. Fig.10 below shows that the force as same gauge pressure is the same as the force of a single PMA. In other words, the force of series PMAs is divided by the number of series sections. From eq.9, we can see that each section will contract by the same contraction ratio (ε) at (p bar). Therefore, the two muscles will act as one long muscle, and its length is the addition of series PMAs. Even the sections are not identical.

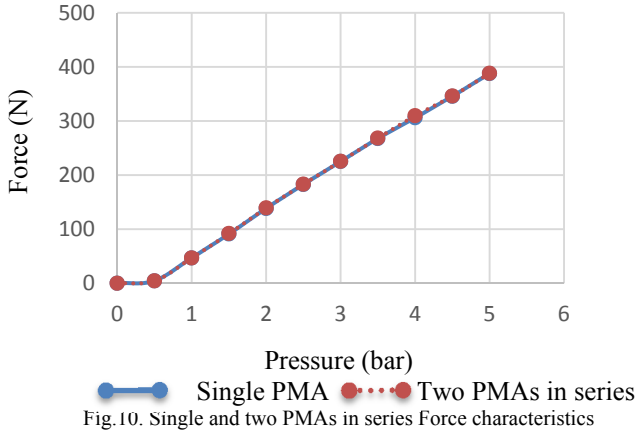

Fig.10. Single and two PMAs in series Force characteristics

Fig.11 illustrates the force characteristic of two 30 cm PMAs in series and of a single 60 cm PMA, and it is clear that the contraction ratio of the 60 cm PMA is similar to the contraction ratio of the two 30 cm series PMAs. Therefore, the force is similar too.

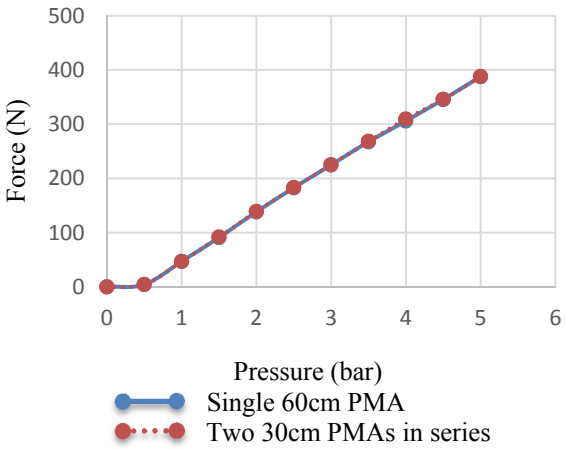

Fig.11. Single long PMA and two PMAs in series Force characteristics

VI. MODELLING OF THE ARM FREE END ANGLE

The pneumatic muscle actuator arm has a smooth bending behaviour when it is actuated by air [26]. There have been a number of researches done on curvature [6, 26]. In this paper the free end angle of a 4-PMAs 30 cm arm shown in fig.7 is studied as a function of actuated air pressure; no load and load states are considered. Firstly, the experiments are done by recording the initial angle of the free end (α), which is equal to (zero) degree due to a straight-line arm. Secondly, all PMAs are actuated by (0.45 bar), then the pressure is increased in one of PMAs in the corners. The arm will then bend into another position, depending on the amount of (p) in the muscle and α is recorded each time. Fig. 12 shows the contraction arm under actuation from certain pressure between (0-5) bar.

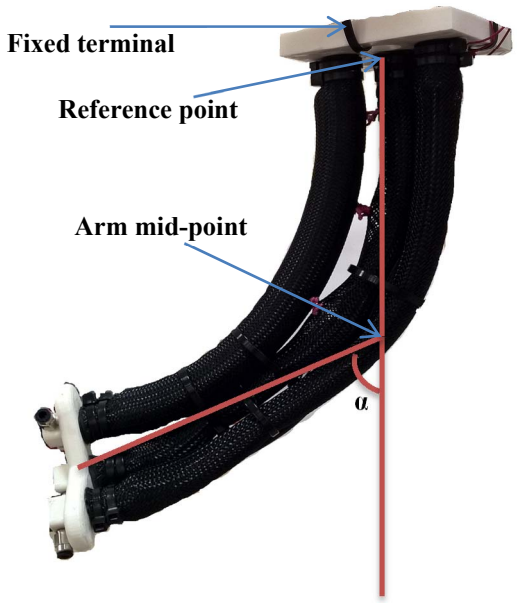

Fig.12 One PMA pressurized arm with α degree angle.

The maximum angle value (α_{max}) depends on the amount of the attached load (w) to the arm end. Table.1 below shows different maximum angles with different load values.

Table.1 maximum angle with different loads

Load (Kg)	Pressure (bar)	α_{max} (degree)
0.0	3.8	84.333
0.1	3.4	84.0
0.2	3.8	75.5
0.3	3.4	66.0
0.4	3.0	57.0
0.5	2.8	47.0

Fig.13 illustrates the test data for (α) as a function of actuated air pressure in one muscle within the arm at different loads, and it is clear that the maximum angle is reached at high pressure, depending on the load value. From these records, eq.10 models the position angle with any load (w) as a function of pressure (p).

$$\alpha = a + \frac{b}{1+(\frac{p}{c})^d} \tag{10}$$

$$\begin{bmatrix} a \\ b \\ c \\ d \end{bmatrix} = \begin{bmatrix} 85.109 & 68.4155 & -915.4121 & 2145.117 & -1779.245 \\ -86.195 & -69.7074 & 940.9097 & -2210.206 & 1837.185 \\ 1.047706 & 0.1331478 & -4.69328 & 18.98427 & -21.75253 \\ 3.459321 & 0.7990463 & -24.19429 & 84.25137 & -67.01067 \end{bmatrix} \begin{bmatrix} 1 \\ w \\ w^2 \\ w^3 \\ w^4 \end{bmatrix}$$

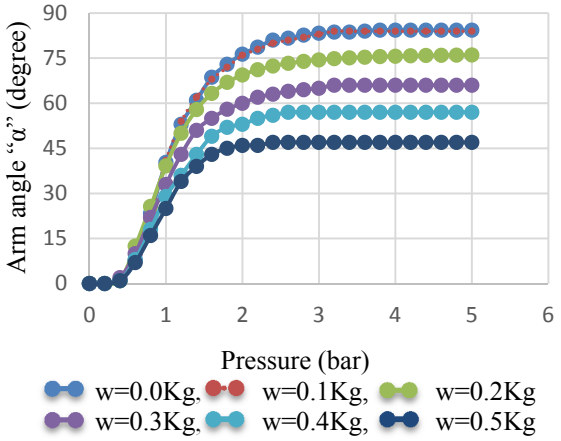

Fig.13. Experimental arm angle

Comparisons between experimental and theoretical data are given in Fig.14 for two states (no load and 0.3 Kg) using eq.10. The figure shows that the slight difference between experimental and theoretical plots can be ignored for (p) equal or more than (2.6 bar).

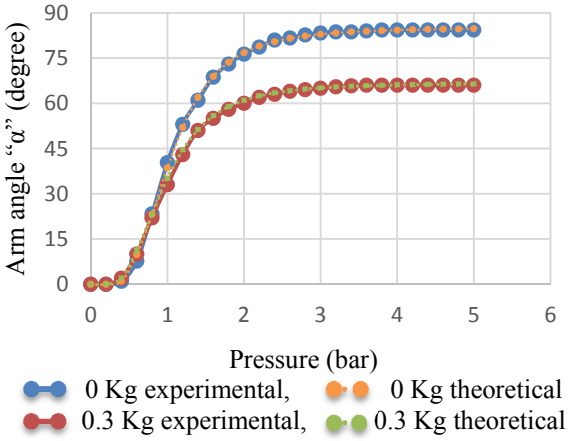

Fig.14. Experimental and theoretical angle value

VII. CONCLUSION

An experimental model for the length of a pneumatic muscle actuator is presented in this paper by two equations.

These equations show minimum error between the model and experimental data for muscles with any nominal length L_0 between 15 cm and 40 cm. On the other hand, calculating the specific zero force pressure in addition to using the shape correction factor, it makes the force model equation a more accurate and substantial match to the experimental data for all muscle lengths under study. Extending the experimental force to an arm of 4-muscles shows that the force of parallel PMAs is four times that of single muscles. On the other hand, the serial muscles provide similar force value whatever the number of series sections. Another important experiment is done for the position of the free end of the arm by calculating the bend angle, through which the base data for position control is established. The mathematical model of this angle is proposed and validated.

As a future work, three-dimensional positions for a continuum arm of any structure could be modelled as a mathematical equation to make the offline and online control of continuum arms more efficient.

ACKNOWLEDGMENT

The authors would like to thank the ministry of higher education/Iraq, University of Basrah, computer-engineering department for providing scholarship support to the first author of this paper.

REFERENCES

[1] E. Kelasidi, G. Andrikopoulos, G. Nikolakopoulos, and S. Manesis, "A survey on pneumatic muscle actuators modeling." pp. 1263-1269.

[2] S. Davis, N. Tsagarakis, J. Canderle, and D. G. Caldwell, "Enhanced modelling and performance in braided pneumatic muscle actuators," *The International Journal of Robotics Research,* vol. 22, no. 3-4, pp. 213-227, 2003.

[3] H. P. H. Anh, "Online tuning gain scheduling MIMO neural PID control of the 2-axes pneumatic artificial muscle (PAM) robot arm," *Expert systems with applications,* vol. 37, no. 9, pp. 6547-6560, 2010.

[4] R. Ranjan, P. Upadhyay, A. Kumar, and P. Dhyani, "Theoretical and Experimental Modeling of Air Muscle," *International Journal of Emerging Technology and Avanced Engineering,* vol. 2, no. 4, pp. 112-119, 4 Apr, 2012.

[5] K. C. Wickramatunge, and T. Leephakpreeda, "Study on mechanical behaviors of pneumatic artificial muscle," *International Journal of Engineering Science,* vol. 48, no. 2, pp. 188-198, 2010.

[6] I. S. Godage, D. T. Branson, E. Guglielmino, and D. G. Caldwell, "Pneumatic muscle actuated continuum arms: Modelling and experimental assessment." pp. 4980-4985.

[7] A. Bartow, A. Kapadia, and I. Walker, "A novel continuum trunk robot based on contractor muscles." pp. 181-186.

[8] W. McMahan, V. Chitrakaran, M. Csencsits, D. Dawson, I. D. Walker, B. A. Jones, M. Pritts, D. Dienno, M. Grissom, and C. D. Rahn, "Field trials and testing of the OctArm continuum manipulator." pp. 2336-2341.

[9] W. McMahan, B. A. Jones, and I. D. Walker, "Design and implementation of a multi-section continuum robot: Air-Octor." pp. 2578-2585.

[10] T. Leephakpreeda, "Fuzzy logic based PWM control and neural controlled-variable estimation of pneumatic artificial muscle actuators," *Expert Systems with Applications,* vol. 38, no. 6, pp. 7837-7850, 2011.

[11] P. K. Jamwal, and S. Q. Xie, "Artificial Neural Network based dynamic modelling of indigenous pneumatic muscle actuators." pp. 190-195.

[12] B.-S. Kang, C. S. Kothera, B. K. Woods, and N. M. Wereley, "Dynamic modeling of Mckibben pneumatic artificial muscles for antagonistic actuation." pp. 182-187.

[13] D. Trivedi, C. D. Rahn, W. M. Kier, and I. D. Walker, "Soft robotics: Biological inspiration, state of the art, and future research," *Applied Bionics and Biomechanics,* vol. 5, no. 3, pp. 99-117, 2008.

[14] I. S. Godage, and I. D. Walker, "Dual Quaternion based modal kinematics for multisection continuum arms." pp. 1416-1422.

[15] T. Zheng, D. T. Branson III, R. Kang, M. Cianchetti, E. Guglielmino, M. Follador, G. A. Medrano-Cerda, I. S. Godage, and D. G. Caldwell, "Dynamic continuum arm model for use with underwater robotic manipulators inspired by octopus vulgaris." pp. 5289-5294.

[16] T. D. C. Thanh, and K. K. Ahn, "Nonlinear PID control to improve the control performance of 2 axes pneumatic artificial muscle manipulator using neural network," *Mechatronics,* vol. 16, no. 9, pp. 577-587, 2006.

[17] B. Tondu, and P. Lopez, "Modeling and control of McKibben artificial muscle robot actuators," *Control Systems, IEEE,* vol. 20, no. 2, pp. 15-38, 2000.

[18] T. Szepe, "Accurate force function approximation for pneumatic artificial muscles." pp. 127-132.

[19] T. Nakamura, and H. Shinohara, "Position and force control based on mathematical models of pneumatic artificial muscles reinforced by straight glass fibers." pp. 4361-4366.

[20] M. More, and O. Líška, "Comparison of different methods for pneumatic artificial muscle control." pp. 117-120.

[21] G. Andrikopoulos, G. Nikolakopoulos, and S. Manesis, "Advanced Nonlinear PID-Based Antagonistic Control for Pneumatic Muscle Actuators, on " *Industrial Electronics, IEEE Transactions,* vol. 61, no. 12, pp. 6926-6937, 2014.

[22] C.-P. Chou, and B. Hannaford, "Measurement and modeling of McKibben pneumatic artificial muscles," *Robotics and Automation, IEEE Transactions on,* vol. 12, no. 1, pp. 90-102, 1996.

[23] S. Davis, and D. G. Caldwell, "Braid effects on contractile range and friction modeling in pneumatic muscle actuators," *The International Journal of Robotics Research,* vol. 25, no. 4, pp. 359-369, 2006.

[24] J. Sárosi, I. Bíró, J. Németh, and L. Cveticanin, "Dynamic modeling of a pneumatic muscle actuator with two-direction motion," *Mechanism and Machine Theory,* vol. 85, pp. 25-34, 2015.

[25] N. Tsagarakis, and D. G. Caldwell, "Improved modelling and assessment of pneumatic muscle actuators." pp. 3641-3646.

[26] I. S. Godage, D. T. Branson, E. Guglielmino, G. A. Medrano-Cerda, and D. G. Caldwell, "Dynamics for biomimetic continuum arms: A modal approach." pp. 104-109.